Prediction of crack propagation using γ-model for through wall cracked Pipes

BY

Shashi Kumar

NIT ROURKELA

A thesis submitted for the award of Master of Technology in Mechanical Engineering

May-2011

Prediction of crack propagation using γ-model for through wall cracked Pipes

A thesis submitted in partial fulfillment of the requirements for the award of Master of Technology in Machine Design and Analysis

BY

Shashi Kumar

209me11987

Under of guidance of

Dr. P.K.RAY

&

Dr. B.B.Verma

Department of Mechanical Engineering
NIT Rourkela
Rourkela

2011

National Institute of Technology

Rourkela

CERTIFICATE

This is to certify that the thesis entitled, **"Prediction of crack propagation using γ-model for through wall cracked Pipes"** submitted by **Mr. Shashi Kumar** in partial fulfillment of the requirements for the award of Master of Technology Degree in **Machine Design and Analysis** at National Institute of Technology, Rourkela (Deemed University) is an authentic work carried out by him under our supervision and guidance. To the best of our knowledge, the matter embodied in the thesis has not been submitted to any other University/Institute for the award of any degree or diploma.

Prof. P.K.Ray

Dept. of Mechanical Engg.

National Institute of Technology

Rourkela-769008

Prof. B.B.Verma

Dept. of Metallurgical and Materials Engg.

National Institute of Technology

Rourkela-769008

Date:

ACKNOWLEDGEMENT

Successful completion of work will never be one man's task. It requires hard work in right direction. I wish to express my deep sense of gratitude and indebtedness to **Prof. P.K.Ray, Dept. of Mechanical Engineering** and **Prof. B.B.Verma**, **Dept. of Metallurgical & Materials Engineering,** N.I.T Rourkela, for introducing the present topic and for their inspiring guidance, constructive criticism and valuable suggestion throughout this project work.

My sincere thanks to our entire Lab mates friends who have patiently extended all sorts of help and their loving support for accomplishing this undertaking. I also thank Mrs. Manila Mallik, Mr. Shamu Hemram and Pawan Kumar for their constant support throughout the project work

Place: Rourkela
Date: 06/06/2011

Shashi Kumar (209ME1187)

Machine Design and Analysis

Dept. of Mechanical Engineering

National Institute of Technology

Rourkela - 769008

ABSTRACT:

The pipe installations occasionally experience high amplitude vibration (Seismic Vibration). This vibration may initiate a new crack or propagate an existing crack. The monitoring of crack becomes more significant if the pipes carry hazardous fluids. The compliance technique is one of the commonly used methods to monitor crack growth in small size specimens. Crack monitoring in compact tension (CT), three point bend bar (TPBB) specimens are generally preferred for fracture toughness laboratory tests and crack monitoring is done using compliance technique. Crack compliance correlations are available for simple geometries. One of the primary objectives at present investigation is to develop γ-model for straight pipes. Gamma function is a variant of factorial function with its arguments shifted by 1. That is if *n* is a positive integer then $\Gamma(n) = (n\text{-}1)!$. The Gamma function is defined for every complex number whose real part is positive and greater than zero. Generally it is given by an integral given as, $\Gamma(z) = \int_0^\infty t^{z-1}e^{-t}dt$ Re (z) >0. This modified γ-model has been proposed to predict crack growth in through wall cracked pipe. Here *t* is replaced by number of cycles *N*. The parameter *z* is chosen in such a way that it becomes a non-dimensional parameter yet representing the properties that affect crack growth and since the integral is finite the value of integral is not Γ(z). The integral was assumed to be equal to a non-dimensional representing crack growth at the end of fixed cycles of loading. Generally fatigue crack growth depends on the initial crack length material properties and dimensions, loading conditions etc. So the non-dimensional parameter is chosen in such a way so as to include all those properties. So the formula for predicting the final crack length at the end of cycle is given as

$\frac{ma_1}{w} = \int_0^N N^{(\frac{ma_0}{w}-1)} e^{-N} dN.$ Here *m* also a non-dimensional parameter whose value remain approximately constant for a given cycle interval. The value of *m* reduces with increase in the value of ΔK. The value of m changes with change in loading condition as well as crack length so $m = \left(\frac{E}{\sigma_{ys}} \times \frac{K_c}{\Delta K} \times \frac{K_{min}}{K_{max}}\right)^e$. Hence it is needed to correlate parameter *m* with parameters like two crack driving forces Δ*K* and K_{max} and with the material parameters plane stress fracture toughness (K_C), modulus of elasticity (E) and yield stress (σ_{ys}). Fatigue crack growth depends on both Δ*K* and K_{max} in order to consider effects of mean stress. However, this may not take care of the large deformation that occurs during the loading of specimens/components. In case of pipes, additional difficulties arise due to geometric softening or hardening during the deformation process. However for pipes no such correlation is available so using γ-model we can predict the next incremented depth of crack for pipe.

γ-model has also been applied on single edge notch (tension) SENT specimen and shows results are in good agreement with the experimental results for the SENT specimen. The variation is primarily due to experimental errors or other errors arising due faulty reading data and human error. This method is easy to interpret and less time consuming in successfully predicting crack with good degree of accuracy.

Keywords: Crack length measurement, Fatigue crack growth, Stress intensity factor range, fracture toughness, γ-model.

Contents

Figures

Tables

Nomenclature

K	Stress intensity factor
K_{max}	Maximum stress intensity factor in a cycle
K_{min}	Minimum stress intensity factor in a cycle
ΔK	Stress intensity factor range
$\Delta K_{\ i}$	Stress intensity factor range with respective K_{max}
R	Loading ratio or stress ratio
a	Crack depth
L	Straight crack length
Θ	Crack half-circumferential angle
B	Specimen thickness
W	Specimen with
σ_{max}	Maximum stress in a cycle
R_i	Inner radius of pipe
R_o	Outer radius
t Or w	Thickness of pipe
m	Non- dimensional parameter
σ_{ys}	Yield stress
K_c	Fracture toughness
σ_{ut}	Ultimate strength
E	Young's Modulus

Chapter 1

Introduction

1. INTRODUCTION

1.1. Background

Fatigue is defined as the process of progressive localized permanent structural change occurring in a material subjected to conditions that produce fluctuating stresses at some point or points and that may culminate in cracks or complete fracture after a sufficient number of fluctuations. Actually it is behavior of materials under cyclic loading. The stress value in case of fatigue failure is less than ultimate tensile stress and may be below yield stress limit of the material. Generally, fatigue loading implies cyclic variation of stress and strain in a component. The subject of strength of materials is mostly concentrated on the static loading and failure of components in an overload situation. In a dynamic world, however, failure occurs at stresses much lower than the material's ultimate strength. This phenomenon of components, failing at relatively low stresses, came as quite a surprise to most engineers in the early years of metal component design. The other frustrating aspect is that the material exhibited no sign of its tiredness or fatigue and could fail without much warning.

- Pipe installation in industries carries hazard materials in that the disasters could be in the form of fire or serious consequences.
- Piping installation also supsetable due to change in Hoop stress that also they experiences due to high amplitude vibration. One the great technique leak-before-break (LBB) design criteria for through wall carked pipe (TWC) which is based on fracture mechanics concepts are being adopted for fail-safe design criteria The LBB demonstration which is based on fracture mechanics requires information on the initial size of a defect, initiation of crack growth from the inherent defect and subsequent crack growth rates.

- Crack initiation occurs due to fatigue, localize corrosion, slip induced (purity material) and geometry defect.
- The monitoring of crack can be by putting strain gauge or by some other method like alternating current potential difference (ACDP) it may not be always possible.
- These installations are very expensive and life estimation is very essential, if initial crack is sensitive. The crack growth behavior can be known by non-destructive test such as Phase array method, Eddy current testing, Ultrasonic testing, corrosion mapping etc. and the only possible by using certain model. These models may be based on some experimental work or empirical correlation basis.
- Several crack monitoring model are available such as Forman et, Walker, Paris –Erdogan are not meant for Pipe model.

1.2. Fatigue Failure- Mechanism

Often machine members subjected to repeated or cyclic stressing are found to fail when the actual maximum stresses are below the ultimate strength of the material, and quite frequently at stress values even below the yield strength. The most distinguishing characteristic is that the failure occurs on repetition of stress cycles on several occasions. Fatigue is estimated to cause 90% of all failures of metallic structures or components such as bridges, aircraft, machine components, etc. are occurring under fluctuating / cyclic stresses, failure can occur at loads considerably lower than tensile or yield strengths of material under a static load.

Fatigue failure begins with a small crack; the initial crack may be so minute and cannot be detected. The crack usually develops at a point of localized stress concentration like discontinuity in the material, such as a change in cross section, a keyway or a hole. Once a crack is initiated, the stress concentration effect become greater and the crack propagates.

Consequently the stressed area decreases in size, the stress increase in magnitude and the crack propagates more rapidly. Until finally, the remaining area is unable to sustain the load and the component fails suddenly. Thus fatigue loading results in sudden, unwarned failure.

Fatigue failure is brittle-like relatively little plastic deformation even in normally ductile materials by applied stresses causing fatigue may be axial (tension or compression), flexural (bending) or torsional (twisting). It proceeds in three distinct stages:

* Crack initiation in the areas of stress concentration (near stress raisers),
* Incremental crack propagation
  → Oscillating stress... Crack grows, stop growing, grows, stops growing... with crack growth due to tensile stresses, and
* Final catastrophic failure.

The macro mechanisms of fatigue failure of above three steps are given below:

* Crack initiation
  → Areas of localized stress concentrations such as fillets, notches, key ways, bolt holes and even scratches or tool marks are potential zones for crack initiation.
  → Crack initiation at the sites of stress concentration (micro cracks, scratches, indents, interior corners, dislocation slip steps, etc.). Quality of surface is important.
  → Crack also generally originates from a geometrical discontinuity or metallurgical stress raiser like sites of inclusion.
  → Due to result of the local stress concentrations at these locations, the induced stress goes above the yield strength (in normal ductile materials) and cyclic plastic straining results due to cyclic variations in the stresses. On a macro scale the average value of the induced stress might still be below the yield strength of the material.

* Incremental crack propagation

→ Stage I: initial slow propagation along crystal planes with high resolved shear stress. Involves just a few grains, and has flat fracture surface.

→ Stage II: In the second stage: faster propagation perpendicular to the applied stress. Crack grows by repetitive blunting and sharpening process at crack tip. Rough fracture surface is shown in second stage.

→ As the size of the crack increases the cross sectional area resisting the applied stress decreases and reaches a thresh hold level at which it is insufficient to resist the applied stress.

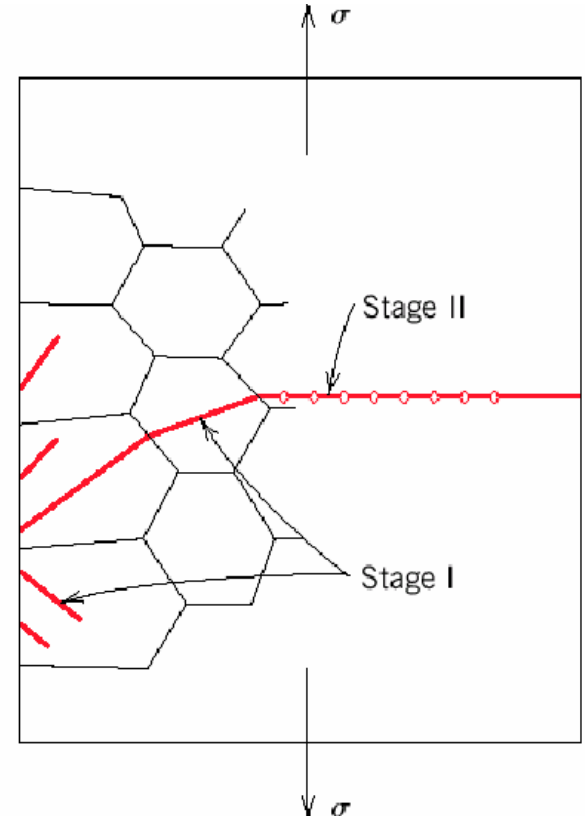

Fig. 1.2 Stages of crack propagation [1].

* Final catastrophic failure

As the area becomes too insufficient to resist the induced stresses any further a sudden fracture results in the component because Crack eventually reaches critical dimension and propagates very rapidly.

1.3. Factors that affects fatigue are

* Geometry

Geometries do not have fatigue strength. Different geometries affect fatigue strength and fracture mechanics parameters, chemistry and mechanical properties are the same. Notches and variation in cross section throughout a part lead to stress concentrations where fatigue cracks initiate. To account for stress concentration effect, the actual maximum stresses have been determined either experimentally or by using more sophisticated stress analysis methods, such as finite element analysis, for common types of geometric features. Based on such calculations the geometric stress concentration factors (K) are determined for these types of features. The stress concentration factor is defined as

$$K = \frac{highest\ value\ of\ actual\ stress\ on\ fillet\ notch\ hole\ etc}{calculated\ stress\ for\ their\ minimum\ crossection}$$

The value of the factor K varies from 1 to about 3 in most cases. $K= 1$ means no stress concentration, that is, calculated value of stress = actual value of stress. When $K = 3$, the actual stress is three times the calculated value.

* Surface quality

Surface roughness cause microscopic stress concentrations that lower the fatigue strength. This much lower fracture strength is explained by the effect of stress concentration at microscopic flaws. The applied stress is amplified at the tips of micro-cracks, voids, notches, surface scratches, corners, etc. that are called stress raisers. The magnitude of this amplification depends on micro-crack orientations, geometry and dimensions [1]. This much lower fracture strength is explained by the effect of stress concentration at microscopic flaws. The applied stress is amplified at the tips of micro-cracks, voids, notches, surface scratches, corners, etc.

that are called stress raisers. The magnitude of this amplification depends on micro-crack orientations, geometry and dimensions. Compressive residual stresses can be introduced in the surface by e.g. shot peening to increase fatigue life. Such techniques for producing surface stress are often referred to as peening, whatever the mechanism used to produce the stress. Low Plasticity Burnishing, Laser peening, and ultrasonic impact treatment can also produce this surface compressive stress and can increase the fatigue life of the component. This improvement is normally observed only for high-cycle fatigue. In Figure 1.3.1 it can be observed.

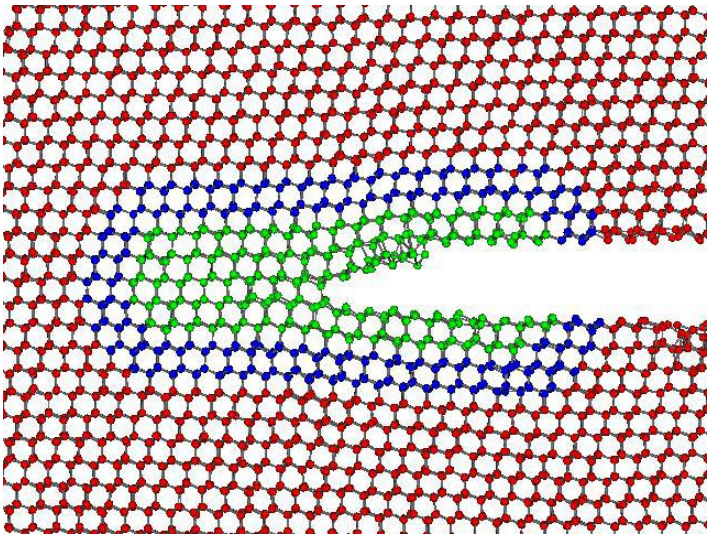

Fig. 1.3.1 Surface crack formation by N. Bernstein &D. Hess, NRL [1].

* Cyclic stress state

Cyclic stresses are characterized by maximum, minimum and mean stress, the range of stress, the stress amplitude, and the stress ratio. Depending on the complexity of the geometry and the loading, one or more properties of the stress state need to be considered, such as stress amplitude, mean stress, biaxiality, in-phase or out-of-phase shear stress, and load sequence.

Mean stress: $\sigma_m = (\sigma_{max}+\sigma_{min}) / 2$

Range of stress: $\sigma_r = (\sigma_{max} - \sigma_{min})$

Stress amplitude: $\sigma_a = \sigma_r /2 = \sigma_{max} - \sigma_{min})/2$

Stress ratio: $R = \sigma_{min}/\sigma_{max}$

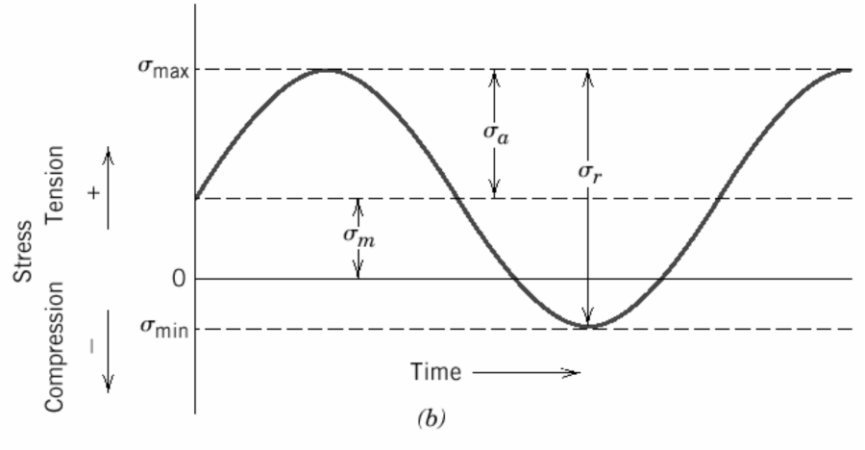

Fig. 1.3.2 Characterization of cyclic stress

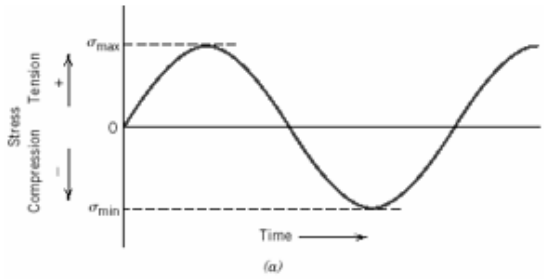

Fig. 1.3.3 Periodic and symmetrical about

Zero stress

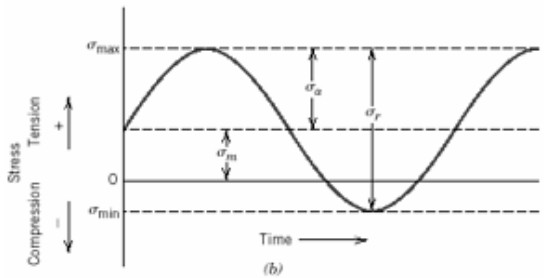

Fig. 1.3.4 Periodic and asymmetrical About zero stress

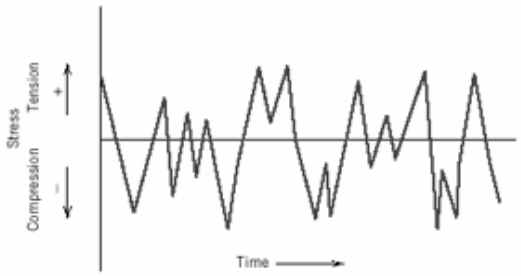

Fig. 1.3.5 Random stress Fluctuations

* Material Type

Fatigue life, as well as the behavior during cyclic loading, varies widely for different materials, e.g. composites and polymers differ markedly from metals.

* Residual stresses

Residual stresses are stresses that remain after the original cause of the stresses (external forces, heat gradient) has been removed. They remain along a cross section of the component, even without the external cause. Residual stresses occur for a variety of reasons, including inelastic deformations and heat treatment. Heat from welding may cause localized expansion, which is taken up during welding by either the molten metal or the placement of parts being welded. Welding, cutting, casting, and other manufacturing processes involving heat or deformation can produce high levels of tensile residual stress, which decreases the fatigue strength.

* Size and distribution of internal defects

Casting defects such as gas porosity, non-metallic inclusions and shrinkage voids can significantly reduce fatigue strength.

* Grain size

Grain size has its greatest effect on fatigue life in the low-stress, high-cycle regime in which stage 1 cracking predominates. In high stacking-fault-energy materials (such as aluminum and copper) cell structures develop readily and these control the stage 1 crack propagation. Thus, the dislocation cell structure masks the influence of grain size, and fatigue life at constant stress is insensitive to grain size. However, in a low slacking-fault-energy material (such as alpha brass) the absence of cell structure because of planar slip causes the grain boundaries to control the rate of cracking. In this case, fatigue life is proportional to grain diameter.

* Temperature

High body temperature per se causes fatigue in trained subjects during prolonged exercise in compensable hot environments. Furthermore, time to exhaustion in hot environments in trained subjects is inversely related to the initial level of body temperature and directly related to the rate of heat storage.

* Environment

Corrosion fatigue is fatigue in a corrosive environment. It is the mechanical degradation of a material under the joint action of corrosion and cyclic loading. Nearly all engineering structures experience some form of alternating stress and are exposed to harmful environments during their service life. The environment plays a significant role in the fatigue of high strength structural materials like steels, aluminum alloys and titanium alloys. Materials with high specific strength are being developed to meet the requirements of advancing technology.

1.4.PROBLEM STATEMENT

1.4.1. Four Point bend Method

Four point bending (FPB) is a cornerstone element of the beam flexure portion of a sophomore-level mechanics of materials course. The FPB lecture has traditionally developed the theory from free body diagram through beam deflection, with related homework problems providing analytical practice. In FPB method Beam flexure represents one of the three most common loading categories for mechanical systems. As such, it is on the syllabi of nearly all sophomore-level mechanics of materials courses, including the mechanical engineering technology course under consideration here. Within the lecture setting, FPB theory is developed from free-body diagram through beam deflection. This theory is reinforced by analytical practice solving related homework problems [2-4]. By this FPB the result to

experimentally and analytically verify and Validated beam flexure theory [4]. According to the convention specified in ASTM D6272-00 transverse vertical loads are applied to horizontal beams such that a constant bending moment results between the two inner load locations [4]. Figure 1.4.1, shows the corresponding loading diagrams, from free-body to bending moment.

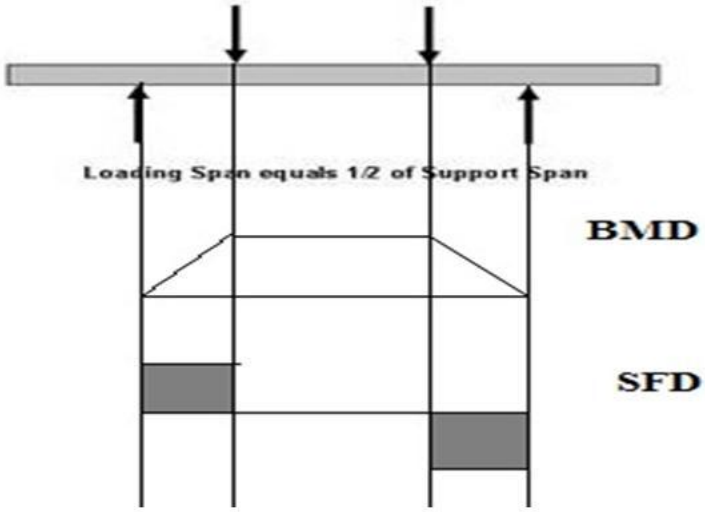

Fig. 1.4.1: Example of Free Body, Distributed Load, and Moment diagrams for the laboratory experiment on four point bending.

1.4.2. Fatigue crack initiation

Fatigue crack initiation strongly depends on the initial crack depth and load ratio. Number of cycles to crack initiation can be predicted well by evaluating local stress based on a fracture mechanics approach. For the typical stress range expected in the piping of Pressurized Heavy Water Reactor (PHWR), the number of cycles to crack initiation is very large compared to the expected number of cycles.

Initiation of the crack strongly dependents on the material condition, state of stress ahead of the crack tip. The mechanism of initiation is due to development of slip planes in the material, which coincide with maximum shear stress, and become sites for crack initiation. This development of slip bands depends on the magnitude of stress range at the notch tip. The slip

plane formation in the material may take place irrespective of the nature of the stress, provided the magnitude of the stress range applied is sufficient for creation of a slip band [5]. It has also been found that for a given stress range, the number of cycles required for crack initiation dependents on the initial crack or notch.

1.4.3. Fatigue crack growth

The alloy 316L (S31603) is molybdenum-bearing austenitic stainless steels. The general corrosion and pitting/crevice corrosion resistance of this alloy is superior to the conventional chromium-nickel austenitic stainless steels such as alloy 304, especially when oil and gas or hazardous fluid carries through large-diameter pipelines. It is well established that early damage may occur in service due to the fluctuations in the internal operating pressure, as well as the variation in external loads. The need of transporting oils and gases for various industries demands quality steels for large-diameter pipelines. It is also worth to mention that the fatigue crack growth can be accelerated by an aggressive environment [6-8]. The effects of stress ratio on the fatigue crack growth behavior are widely available for standard specimens [9]. Fatigue crack growth behavior depends on the stress state at the notch tip, the geometry of the component, the shape and size of the notch and loading conditions. Therefore, the fatigue crack initiation and growth behavior of small laboratory specimens may differ from that of actual piping and their components. A few researchers [10–11] have carried out fatigue crack growth studies on full scale piping components for Light water reactor (LWR) of 219 mm outer diameter and thickness 15 mm has Fracture resistance is more as compare to our case like pipe has outer diameter 60 mm and thickness 9 mm.

1.5. Objective

The present investigation to develop a model which can be used to monitor the crack. Formulate model in such a way that it can be directly apply to Pipes. A model becomes strong and effective if it is based on experimental finds or observation. To achieve this objective circumferential notched (straight notched) and subsequent pre-crack pipe were tested on the dynamic loading condition and crack growth is monitor with the help of COD gauge and a low magnification microscope or optically. It is especially important in case of nuclear power plants because of the application of leak-before-break (LBB) concept which involves detailed integrity assessment of primary heat transport piping systems taking into account the postulated cracks, these cracks occurring due to oil such as natural uranium fuel and gases.

1.6. Problem Approach

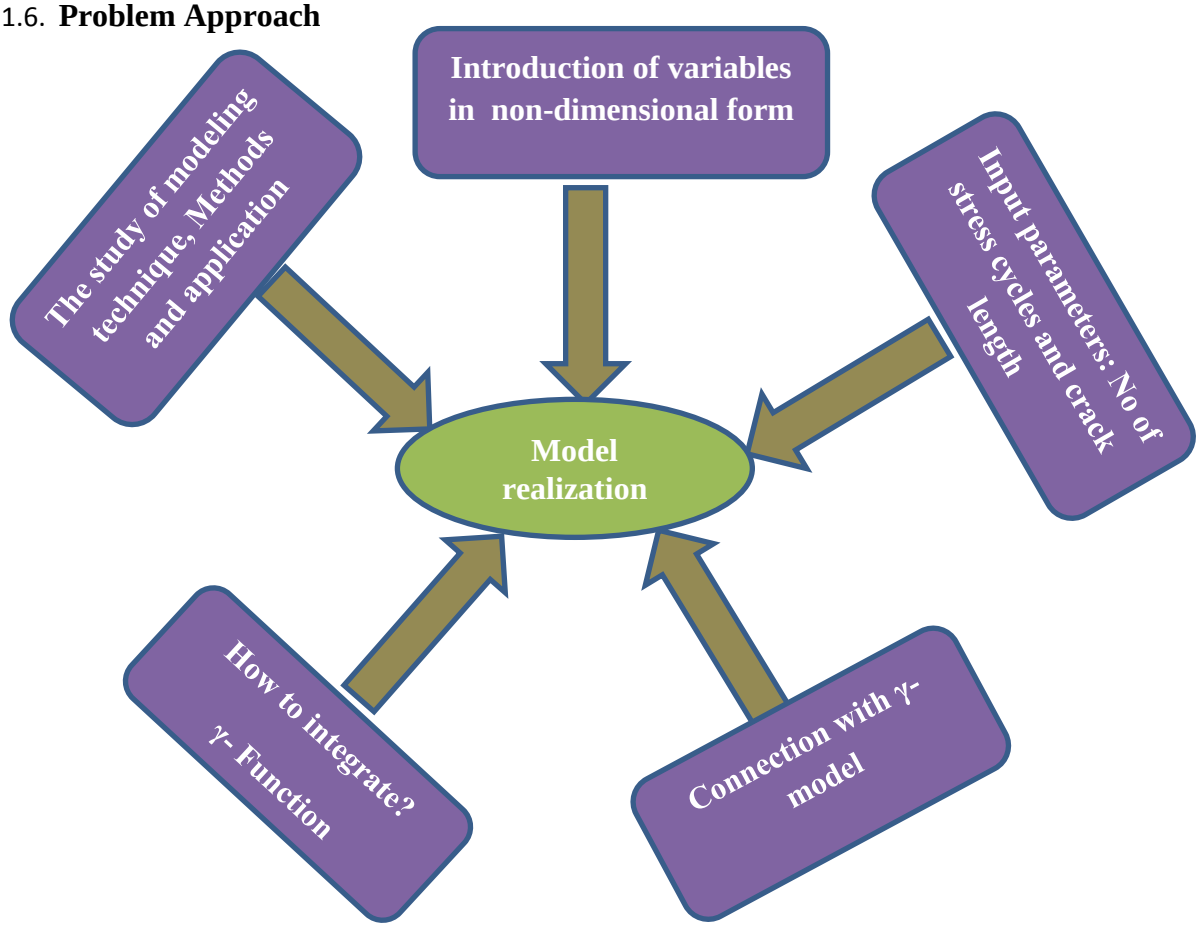

Fig.1.6.1 γ-model

1.6.1. **Modeling Technique**

Fatigue plays very important role in piping systems and may lead to crack initiation from either the highly stressed regions or the flaws. The crack initiation and subsequent propagation must be avoided in any piping system. These pipe installations occasionally experienced high amplitude vibration (e.g. seismic vibration). These vibrations may initiate /extent the exiting cracks. The monitoring of crack becomes more significant if the installation of pipe is carrying hazards fluid. The design criteria for through wall carked pipe (TWC) is Leak-Before-Break (LBB) based on fracture mechanics concepts are being adopted for fail-safe design criteria. The LBB demonstration which is based on fracture mechanics requires information on the initial size of a defect, initiation of crack growth from the inherent defect and subsequent crack growth rates. The nature of crack will grow and penetrate the wall thickness under fatigue loading. Thereafter, the crack will grow in the circumferential direction under cyclic loading. Correlations are available for compact tension (CT), three-point bend (TPB) and some other geometry of small laboratory specimens, so we proposed gamma model (γ-model) to account for the tremendous amount of uncertainty and difficulty in predicting to measure the crack growth. The crack monitoring by this technique requires a gamma function, correlating the crack length with respective stress cycles. However, for pipes no such correlations are available, although fracture tests are widely carried out on these components. One of the primary objectives of the project is to develop gamma correlations for straight pipes. Conventionally, gamma model correlation is developed by generating gamma function vs. crack length data.

Several definitions have been proposed for the gamma function. Harald Bohr and Johannes Mollerup then proved what is known as the Bohr–Mollerup theorem: that the gamma function

is the unique solution to the factorial recurrence relation that is positive and accurate and logarithmically convex for positive value of in terms of *z* and whose value at 1 is 1 (a function is logarithmically convex if its logarithm is convex). The Bohr–Mollerup theorem is good and useful because it is relatively easy to prove logarithmic convexity for any of the different formulas used to define the gamma function. By taking things further it seem to be, instead of defining the gamma function by any particular formula, we can choose the conditions of the Bohr–Mollerup theorem as the definition, and then pick any formula we like that satisfies the conditions as a starting point for studying the gamma function. The definite integral γ-function can be utilized to monitor crack in a body and is defined as follows;

$$\Gamma(z) = \int_0^{\infty} t^{z-1} e^{-t}\, dt, \text{ Re } (z) > 0.$$

Here *t* represents number of stress cycles *N*. The parameter *z* is chosen in such a way that it becomes a non-dimensional parameter yet representing the properties that affect crack growth. The value of integral is equal to a non-dimensional parameter representing crack growth at the end of fixed cycles of loading. Generally, fatigue crack growth depends on the initial crack length, specimen dimensions, material properties and loading conditions. The non-dimensional parameter is developed to include all these variables. The γ-model is completely new technique introduces for getting next depth of crack by introducing the non-dimensional number and curve fitting value or varying exponent values. The good thing of this technique we can get easily depth of crack without going through scanning electron microscopic (SEM).

Chapter 2

LITERATURE REVIEW

2. LITERATURE REVIEW

2.1. Fatigue Crack Growth Rates in Pipeline Steels Using Curved M(T) Specimens

According to this literature survey, 316L austenitic steel has good fatigue properties in compare to ferrite-pearlite steel. In this paper they have taken two steel one of ferrite-pearlite steel without banding has better fatigue properties than second ferrite-pearlite banded steel by fatigue rate (FCGR) behavior (d*a*/d*N*). Uncertainty or immeasurably in the fatigue crack growth rates was analyzed by attributing the entire fatigue scatter to the Paris law parameter *C* and exponent *n.* The Finite Element Analysis (FEA) based simulation model, which is based on the curved geometries, has good compliance relationship and more accurately predicted both fatigue crack growth data and true crack lengths. Never the less, according to the ASTN E647-05 compliance relationship accurately predicted the crack length for the M (T) geometry, although its use leads to slightly conservative fatigue crack growth result and a slight over estimation of the true final crack length. In this paper FCGR evaluation is investigated. The common way to monitor FCGR tests is to use a clip gage mounted in the specimen notch and calculate the crack length using the specimen compliance via the crack mouth opening displacement (CMOD). This method has the advantage of generating data directly during the fatigue test without any stop-and-start process, and it is based entirely on the compliance relationship technique. The possible effects of using curved specimens of pipe, machined directly from the full-thickness pipeline are also examined. The pipeline industry usually uses flattened or machined small-size specimens, such as single-edge notched [12, 13–15], compact tension (C (T)) [8, 16, 17] or three-point bending [18] specimens. To get a better measurement of the compliance, CMOD vs. load curve were excluded throughout top and bottom portions of the pipe, with only the interior points fitted. This should prevent nonlinearities encountered through phenomena such as crack closure from affecting the slope of the curve. Furthermore the most, points were collected on both sides of the loading and unloading curves in order to average possible hysteresis effects.

The fatigue tests were conducted at room temperature using a computerized servo hydraulic fatigue machine with a loading ratio $\frac{Kmin}{Kmax}$, (where $Kmin$ and $Kmax$ are calculated from the minimum and maximum applied load, respectively) equal to 0.4 at a frequency of 10 Hz. Three

tests were conducted on X52 steel and two tests were conducted on Grade B steel. The stress intensity factor range ΔK was calculated according to the following equation from Tada et al. [19]:

$$\Delta K = \frac{\Delta P}{BW}\sqrt{\pi(R_i\theta)}.F(\theta)$$

$$F(\theta) = 1+7.5(\theta/\pi)^{1.5} - 15.0(\theta/\pi)^{2.5} + 33.0(\theta/\pi)^{3.5}$$

$\theta = tan^{-1}(\frac{a}{R_i})$ Where

a=half crack length,

θ =crack half-circumferential angle,

R_i = mean radius, (R_i = (OD/2) - pipeline thickness/2))

This equation is valid when θ <110° [19].

The CMOD predicted from the model as, identified as the relative displacement across the notch edges along the center line of the model, and corresponded to the CMOD gage attachment points in the experimental tests. Whereas by symmetry the CMOD is the same for both sides of the flat specimen, the pipe curvature causes the CMOD to vary between the outer diameters (OD) and inner diameters (ID) of the curved model. In accordance with the ASTM E647-05 expression used to predict the crack length as a function of compliance.

$$\frac{2a}{W} = c_1x + c_2x^2 + c_3x^3 + c_4x^4$$

Where a = half crack length, W=specimen width, C_0,C_1,C_2,C_3, C_4 are compliance coefficients

$$x = 1 - e^{(-\sqrt{(EBC_M+\eta)}(EBC_M-\eta+C_1\eta+C_2\eta^{C_3}))/2.141}$$

E = Young's modulus, B = specimen thickness, C_M = measured compliance (CMOD/Load) and

$\eta = 2y/W$, where y is the distance from the carck to point where the CMOD is measured (half of the gauge length) [20].

2.2. Crack initiation and growth behavior of circumferentially cracked pipes under cyclic and monotonic loading

Studies have been carried out on carbon steel pipes to demonstrate the leak before break design criterion and validate the analytical procedures. Fatigue crack initiation, fatigue crack growth rate and fracture resistance behavior of the pipes have been experimentally and analytically evaluated and it shows good result. The tests have been carried out on pipes 219 mm outer diameter and wall thickness 15 mm having a part through notch in the circumferential direction or its curve length of Light water reactor (LWR) has Fracture resistance is more as compare to our case like pipe has outer diameter 60 mm and thickness 9 mm. The aspect ratios (2c/a) of the notches were 18, 28 and 56. Comparing the experimental and analytical results has validated analytical procedures. It has been observed that the analytical and experimental results are compare well. The fatigue crack growth curve (da/dN~ ΔK) obtained from three point bend (TPB) specimens and pipe tests have been compared with the fatigue crack growth curve in ASME Section XI. The comparison shows that by using the ASME curve in analysis of components will give a conservative result in comparison to the curves obtained from the actual pipe tests. Fracture resistance behavior of the pipe has been observed to be strongly dependent on the load histories to which the pipe has been subjected. Crack growth rate is a function of range of stress intensity factor (ΔK) and this varies along the notch length having a maximum at the middle of the notch (maximum depth) and a minimum at the surface for a given notch aspect ratio is less [21-22].

Crack growth at the surface of the pipe in the circumferential direction has not been observed during the test till the crack has reached through thickness. Some other investigator has also

reported that if the aspect ratio of the notch exceeds 10 or near by 10, crack growth takes place only in the depth direction [23]. Even after crack initiation, the number of cycles required for the crack to grow through-wall is enormously large. The ratio of moment required to cause instability to the moment expected during safe shutdown earthquake (SSE) is more than$\sqrt{2}$, thus satisfying the LBB criterion. Fracture resistance of the pipe strongly depends on the prior load and loading cycles to which the pipe has been subjected.

2.3. Some recent developments on integrity assessment of pipes and elbows. Part I: Theoretical investigations

Integrity assessment of piping components is very essential for safe and reliable operation of power plants. Over the last several decades, considerable work has been done throughout the world to develop a system oriented methodology for integrity assessment of pipes and elbows, mainly for application to nuclear power plants. However, there is a scope of further development/improvement of issues, particularly for pipe bends, that are important for accurate integrity assessment of piping. Considering this aspect, a comprehensive Component Integrity Test Program was initiated in 1998 at Reactor Safety Division (RSD) of Bhabha Atomic Research Centre (BARC), India in collaboration with MPA, Stuttgart, Germany through Indo-German bilateral project. In this program, both theoretical and experimental investigations were undertaken to address various issues related to the integrity assessment of pipes and elbows. The important results of the program are presented in this two-part paper. In the part I of the paper, the theoretical investigations are discussed. Part II will cover the experimental investigations. The theoretical investigations considered the following issues: new plastic (collapse) moment equations of defect-free elbow under combined internal pressure and in plane closing/opening moments; new plastic (collapse) moment equations of through wall circumferentially cracked elbow, which are more accurate and closer to the test results; The

effect of deformation on the unloading compliance of TPB specimen and through wall circumferentially cracked pipe to measure crack growth during fracture experiment. These developments would also help to study the effect of stress triaxiality in the transfer of material J–R curve from specimen to component [24-25].

2.4. Assessment of partly circumferential cracks in pipes

Introducing compressive stress we can solve non-linear stress distribution. Most of the research has been conducted on Finite element analysis to determine stress intensity factor. From the paper "assessment of partly circumferential cracks in pipes" presents a new method for predicting the stress intensity factors around a partly circumferential elliptical surface crack in a pipe. The solution is applicable to structures with both double and single curvature. The technique involves a conformal transform in conjunction with a semi-analytical approach that uses a finite element model to obtain the stress distribution in the undamaged structure. By using an indirect methodology, the model development is simplified and the analysis time is minimized. As such a coarse mesh can be used to obtain solutions for multiple crack geometries. Three examples are presented to verify this methodology. They include a partly circumferential elliptical crack under uniform tension, a pipe subject to a residual stress field, and a problem involving double curvature. For simple loading the solution compares with other published solutions to within 5% for an external crack, and to within 15% for an internal crack. For more complex loading conditions the majority of the solutions were within 5% of other published results at the deepest point, and most solutions at the surface agreed to within 15%. For the problem involving double curvature, the solutions agreed to within 4% for an internal crack, and 15% for an external crack [26-29].

Chapter 3

EXPERIMENTAL DETAILS

3. EXPERIMENTAL DETAILS

3.1. Piping materials

The seamless stainless pipes used in atomic nuclear power plants were supplied by BARC Mumbai. The TP 316L grades of stainless steels are used for conditions free likelihood of inter crystalline corrosion caused by welding. Presence of low carbon in these steels minimizes chromium carbide precipitation and improves resistance to inter crystalline corrosion. They are oxidation resistant up to a temperature of 900°C and are safe for use in the damp industrial or onshore atmospheres. However, in low temperature seawater they offer limited resistance to pitting but are susceptible to crevice attack. Their short- and longtime properties at elevated temperatures are also superior to those of comparable TP 304/304L grades. They find wide applications as pipe and heat exchanger tubes in chemical and petrochemical plant, in boilers, food industry and power plants.

The Tensile properties of flat specimens fabricated from straight pipe were determined by using in accordance with the ASTM E8 standards and is presented in Table 3.1. Summarizes the average values of the mechanical properties data (e.g. stress-strain diagram, yield stress, UTS, % elongation, % reduction in area and young's modulus) measured, that were used in the fracture mechanics evaluation of the experiments. The chemical composition of the piping material, TP 316L, austenitic in structure is presented in Table 3.2. By ASTM A240 and ASME SA-240 specifications. These data are used to normalize the results in such a manner so that the proposed correlation becomes independent of the material parameters which have been shown in Figure 3.1.1.

Table 3.1 Mechanical Properties of SS 316L

Young's modulus(E)	220 GPa
Poisson's ratio	0.3
Yield stress	366MPa
UTS	611MPa

Table 3.2 Chemical compositions of SS 316L

	Percentage by Weight ***(maximum unless range is specified)***
Element	**Alloy 316**
Carbon	0.08
Manganese	2.00
Silicon	0.75
Chromium	16.00/18.00
Nickel	10.00/14.00
Molybdenum	2.00/3.00
Phosphorus	0.045
Sulfur	0.030
Nitrogen	0.10
Iron	Bal.

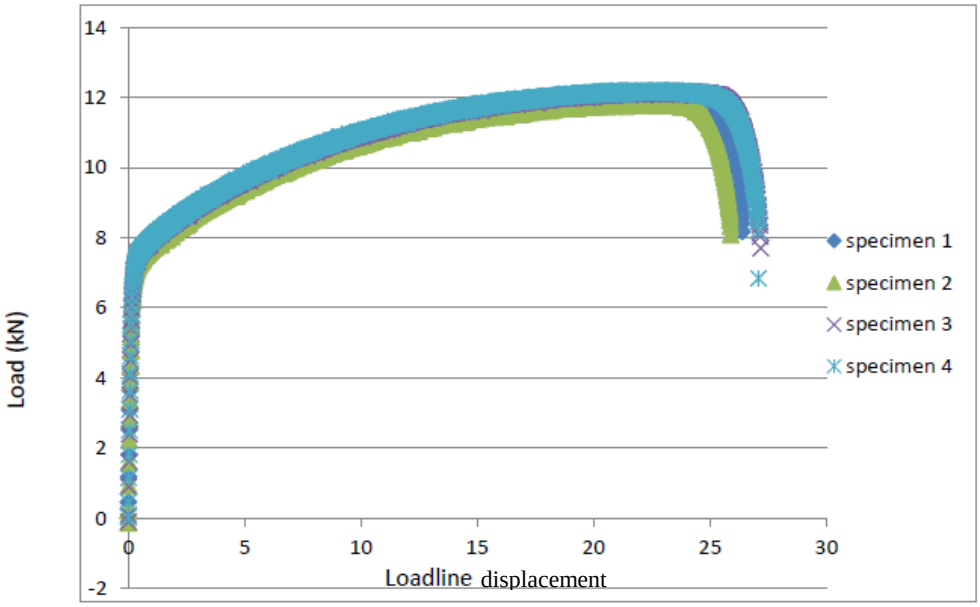

Fig. 3.1.1 Experimental result of Load vs. load line displacement

3.2. Preparation of specimen for FBP test

BARC supplied 60 mm outer diameter and 9 mm wall thickness used in the piping system of Indian Pressurized Heavy Water Reactor (PHWR) have been subjected to FBP tests. Pipe pieces of 505 mm length were used for above tests. Straight surface notches of different depths and notch angle 2θ (45°) were made on the outer circumference by wire EDM maintain notch tip radius 0.8 mm. The detailed dimensions of the specimen and notch are provided in Figure 3.2.1 and Table 3.2.1 respectively.

From literature we have, the pipe specimens with a surface notch are subjected to fatigue loading till the crack has grown through thickness. After this, fracture tests have been carried out on through wall cracked pipes produced by fatigue loading. The final through wall crack size after fatigue has been taken as the initial crack size for the fracture tests.

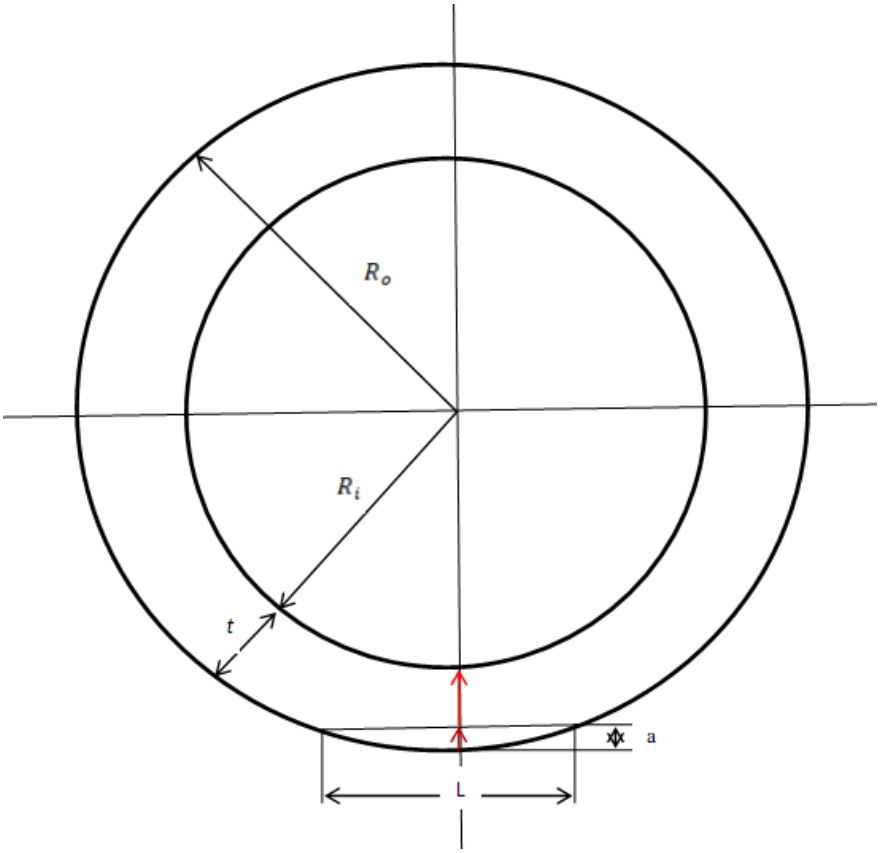

Fig. 3.2.1 Through-wall circumferential flaw in tabular structure

Table 3.2.1 Notch dimension of pipe

Element	Values
R_o (Outer radius)	30 mm
R_i (Inner radius)	21 mm
t (thickness)	9 mm
a (depth of crack)	2.28 mm
L (curve crack length)	23.5 mm

3.3. Test set-up and procedures

The test set up has been shown in figure 3.3.1. It consists of a servo hydraulic loading system, and support for the specimen. A servo hydraulic controlled actuator of ± 250 kN capacity and ± 50mm displacement has been used for loading. The support system consists of two pedestals with two rollers, at an outer span of 465 mm and pair of inner loading rollers with a span of 205 mm, which provides four-point bending. The monitoring of crack was done using a COD gauge and optically using a low magnification microscope.

The notched pipes were pre-cracked till 2 mm by applying condition such as load 36 kN, frequency 5 Hz. Pipe test arrangement constituted loading the pipe under four point bending up to large scale plastic deformation with periodic significant unloading so as to create a beach mark on the crack surface. The unloading path has also given the unloading compliance at that point of deformation. After the test, fractured surface is extracted by Power saw and extracted crack length was examined in scanning electron microscope at various loading stages. This is compared with the theoretical predictions of the proposed compliance correlations. During the test the load was quasi-statically increased under displacement control, until the maximum load was reached. Because of the low compliance of the test rig, unstable crack propagation never occurred. The pipes contained through-wall circumferential notch with help of wire EDM, flaw

tip length about 23.5 mm at an angle 2θ (45°) are made. High toughness of the steel causes large blunting of the flaw tip before the propagation of the crack. The crack opening displacement (COD) was measured by means of a clip gage mounted at the center of the flaw. During the test on through-wall cracked pipes, load line displacement (LLD), load and crack mouth opening dis- placement (CMOD) were recorded. During fatigue testing, the test specimen is subjected to alternating loads until failure. The loads applied to the specimens were defined by either a constant stress range (σ_r) or constant stressamplitude (σ_a). The stress range and stress amplitude are defined in equation (1) and (2), respectively.

$$\sigma_r = \sigma_{max} - \sigma_{min} \quad (1)$$

$$\sigma_a = \frac{\sigma_r}{2} \quad (2)$$

$$\sigma_m = \frac{\sigma_{max}+\sigma_{min}}{2} \quad (3)$$

$$R = \sigma_{min/\sigma_{max}}$$

Where σ_{max} and σ_{min} are maximum and minimum cyclic stress respectively.

$\frac{\sigma}{Y} = \frac{M}{I} = \frac{E}{R}$ From here we find $M = P*a$

Also we have

$$K = \sigma\sqrt{\pi * R * (\theta)} * F(\theta) \quad (4)$$

Where

$$F(\theta) = 1+6.8(\theta/\pi)^{1.5} - 13.6(\theta/\pi)^{2.5} + 20.0(\theta/\pi)^{3.5} \quad (5)$$

Also $2\theta = 45^{\circ}, 60^{\circ}, 90^{\circ}, 100^{\circ}$ *here* $2\theta < 110^{\circ}$

The test specimen was gripped between rollers. This type of loading ensures that the mid-section of the specimen, where the notch is located is subjected to pure bending. The crack

depth all along the notch length at several locations (starting curve length 23.5 mm and depth of crack 2.28 mm) has been recorded during the fatigue crack growth test with the help of crack opening displacement (COD) gauge.

The shape of the crack front has been obtained by measuring the crack depth readings at several locations for a given number of loading cycles. The load and number of cycles corresponding to each crack depth has also been recorded. The load has been measured directly using a strain gauge based load cell. During fracture tests, load line displacement (LLD) has been measured by the inbuilt Linear Variable Differential Transformer (LVDT) of the actuator and load by a load-cell based on strain gauges. Crack mouth opening displacement (CMOD) has been measured by fixing the clip gauge at the center apart from 10 mm from notch length. Console displaying load and displacement at regular interval by the display Waveform. The pre-cracking was mainly done using a hack-saw and the wire EDM which has been shown in figure 3.3.2.The complete experimental setups before bending of pipe shown in figure 3.3.3 and also after cracking and figure 3.3.4. The enlarge view of throughout thickness cracked pipe is shown in figure 3.3.5. The pipes with part through and through-wall notches were fatigue pre-cracked before the fracture tests to ensure sharpness of the crack tip.

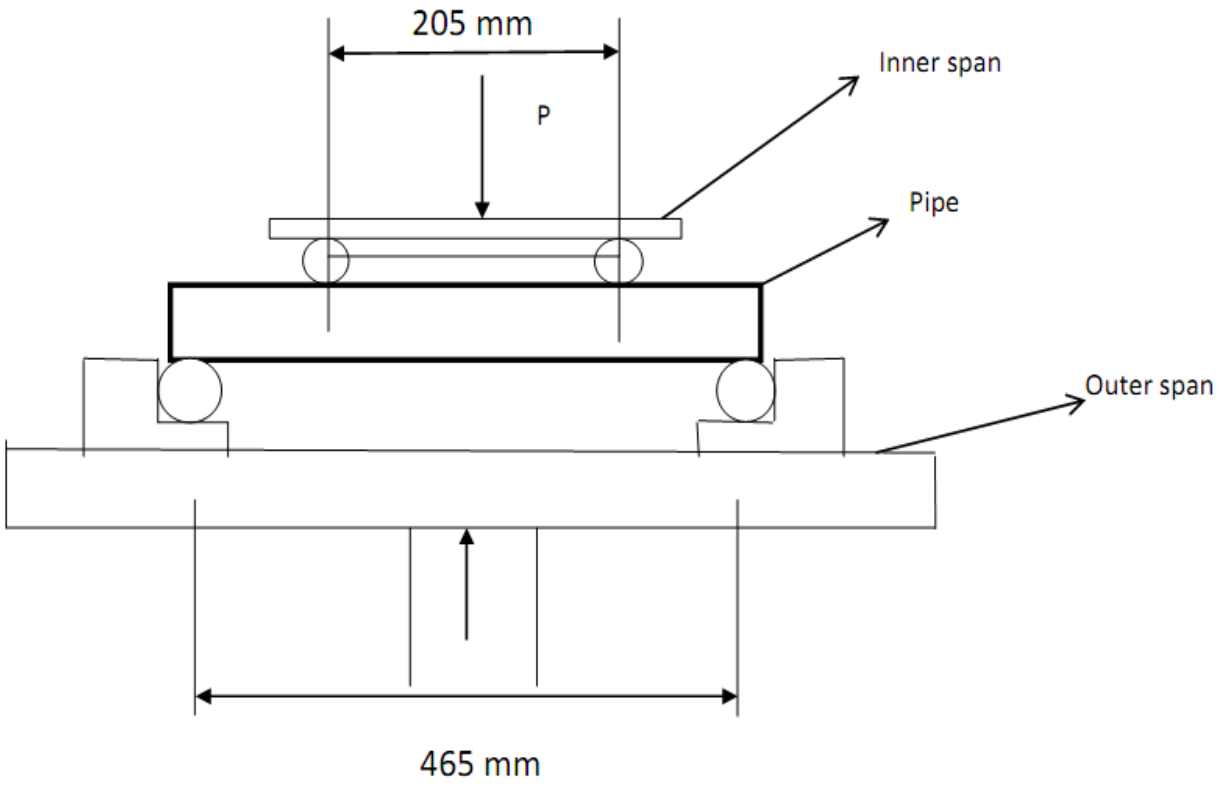

Fig. 3.3.1 four points bend setup arrangement

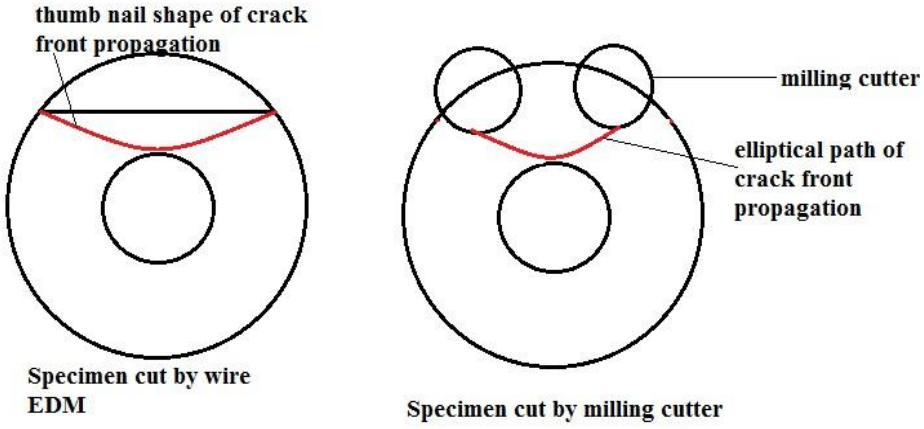

Fig. 3.3.2 Pre-Cracking pattern

Fig. 3.3.3 Schematic diagram of four-point bend test method before crack

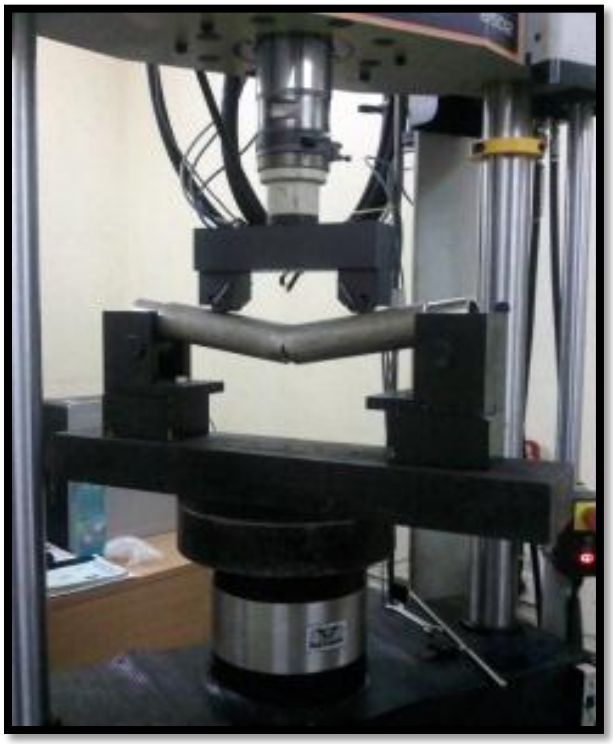

Fig. 3.3.4 Schematic diagram of four-point bend test method after crack

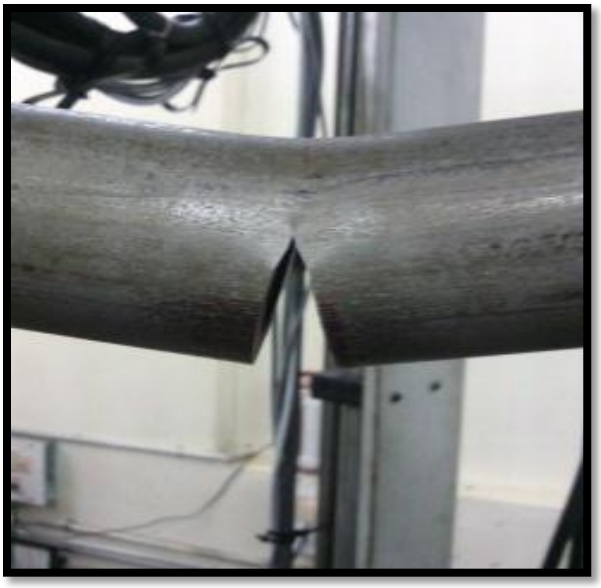

Fig. 3.3.5 Schematic diagram of 316L cracked pipe

3.4. Piping test conditions

Ten sets of pipe of partly circumferential straight crack are tested out at room temperature and air environment under load control mode using sinusoidal waveform loading. The constant amplitude method with stress ratios of 0.1and frequencies in the range of 4–7 Hz has been followed. The typical value of the maximum load of the order of 60KN. Extracted cracked pipe of 10 mm thickness and circumferential crack of 47.7 mm has been taken for scanning electron microscope (Model: JEOL-JSM 6480LV) which has been shown in figure 3.4.1.

Fig. 3.4.1 Cracked sample for SEM

Chapter 4

RESULTS AND DISCUSSIONS

4. RESULTS AND DISCUSSIONS

4.1. Experimental Results

The extension of crack (and crack depth) as function of loading cycle for pipe (1) and (2) are presented in Tables 4.1.1. Initially crack depths have been measured at every 10000 cycles to observe the initiation of the crack from the machined notch. A minimum surface crack length of 0.5 mm was possible to measure by crack opening displacement (COD) gauge. Therefore, in the present study initiation of cracking has been assumed when a crack registered a growth of 0.5 mm. During tests specimens were unloaded and reloaded at a regular interval of 2mm to get beach marks.

The fractured pipe specimen were cut with the help of had milling cutter. This section was then viewed under scanning electron microscope (SEM) in order to see the fracture surfaces. However, beach mark was observed at a few position of crack growth only. This may be due to conducting tests at a fixed load and with no change in the frequency. It was noticed that simply unloading and reloading could not develop the marks on the fracture surface. The possibility of the appearance of beach marks would have been more prominent if the specimen would have been subjected to change of load and/or frequency at regular interval. Three SEM images are presented in Figure 4.1.1. The actual crack depths are also illustrated in those figures. The actual crack depth (measured with the help of SEM is 2.18 mm) and calculated a_c and a_a are also presented on Table. SEM figure 4.1.2 shows that depth of cracks at three points and SEM figure 4.1.3 shows that depth of cracks at different point to view Beach marks. For a given initial crack depth and at constant stress ratio R =0 .1, the maximum crack depth, number of cycles, loads and crack length are shown in figure 4.1.4 (a) - (c). Calculation for Straight pipe is done by taking monitored crack length from experiment which has been shown in Table 4.1.4.

Table 4.1.1 Experimental result of Pipe1 of SS316L

Sl.no.	crack depth calculated chord a_c(mm)	crack depth calculated arc length a_a(mm))	No. of cycles	Load (N)	Monitor Crack length(mm)
1	2.396	2.396	544195	38264	49.467
2	3.153	2.82	567679	38310	50.92
3	3.562	3.467	577741	38349	51.53
4	4.51	5.281	583907	38356	52.09
5	5.49	6.990	595888	38365	52.581
6	6.742	8.575	601392	38360	53.199

Table 4.1.2 Experimental result of Pipe 2 of SS316L

Sl no.	Arc length (curve)mm	crack depth calculated arc length a_a(mm)	*a/t*	Max. load(N)	Monitored Crack length (mm)	*N* (No. of cycles)
1	25.4	2.60	0.28	38264	49.46	94195
2	28	3.20	0.355	38310	50.92	117679
3	34	4.58	0.508	38349	51.53	127741
4	38.5	5.96	0.662	38356	52.09	133907
5	42	7.05	0.783	38360	52.58	145880
6	46	8.390	0.932	38360	53.199	151392

Table 4.1.3 Experimental result of Pipe 3 of SS316L

Sl no.	Arc Length (curve) mm	a_a (mm)	a/t	Max.load	Monitored Crack length(mm)	*N* (No. of cycles)
1	27.5	3.096	0.344	38343	51.91	125876
2	31.5	4.039	0.44	38304.4	52.33	4510
3	35.5	5.096	0.566	38325	52.79	4399
4	39.5	6.26	0.696	38304.1	53.28	4193
5	43.5	7.54	0.837	38377	53.71	3241
6	47.5	8.916	0.99	38351.6	54.07	2137

Table 4.1.4 Experimental result of Straight Pipe1 for different parameter

Sl no.	a_c(crack depth)	Θ	Θ in Radian	smax	F(Θ)	Kmax	Δk	l=[(E*Kc*Kmin)/(sys*Δk*Kmax)]
1	2.2396	22.5	0.392625	241	1.239123	48.06231393	43.25608254	500.2612981
2	2.844	25.15	0.438868	241	1.276204	52.33453965	47.10108569	459.4234652
3	3.336	27.27	0.475862	241	1.306456	55.78744686	50.20870218	430.9879177
4	3.876	29.45	0.513903	241	1.338082	59.37784012	53.4400561	404.9274192
5	4.466	31.66	0.552467	241	1.370677	63.06519242	56.75867318	381.2517592
6	5.111	33.94	0.592253	241	1.404888	66.92628533	60.23365679	359.2566872
7	5.814	36.27	0.632912	241	1.440501	70.93925816	63.84533235	338.9338454
8	6.581	38.682	0.675001	241	1.478129	75.17370154	67.65633138	319.8421132
9	7.418	41.172	0.718451	241	1.517878	79.64106471	71.67695824	301.9009809
10	8.333	43.762	0.763647	241	1.560326	84.40402773	75.96362496	284.8645521
11	9.33	46.46	0.810727	241	1.605907	89.50746511	80.5567186	268.622461

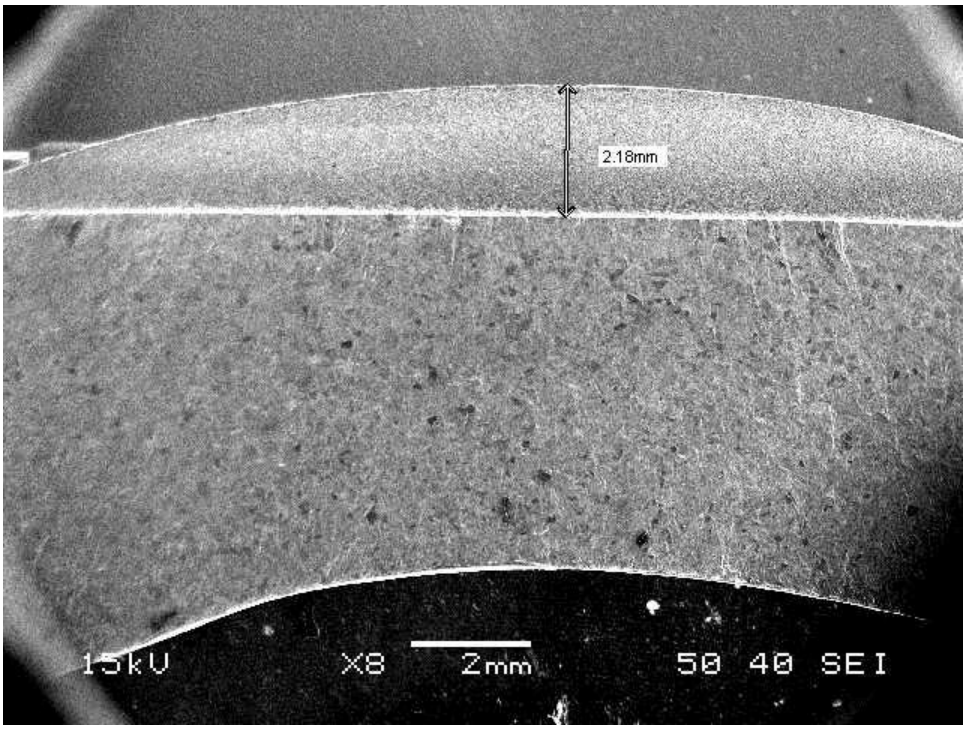

Fig. 4.1.1 SEM, Actual depth of crack

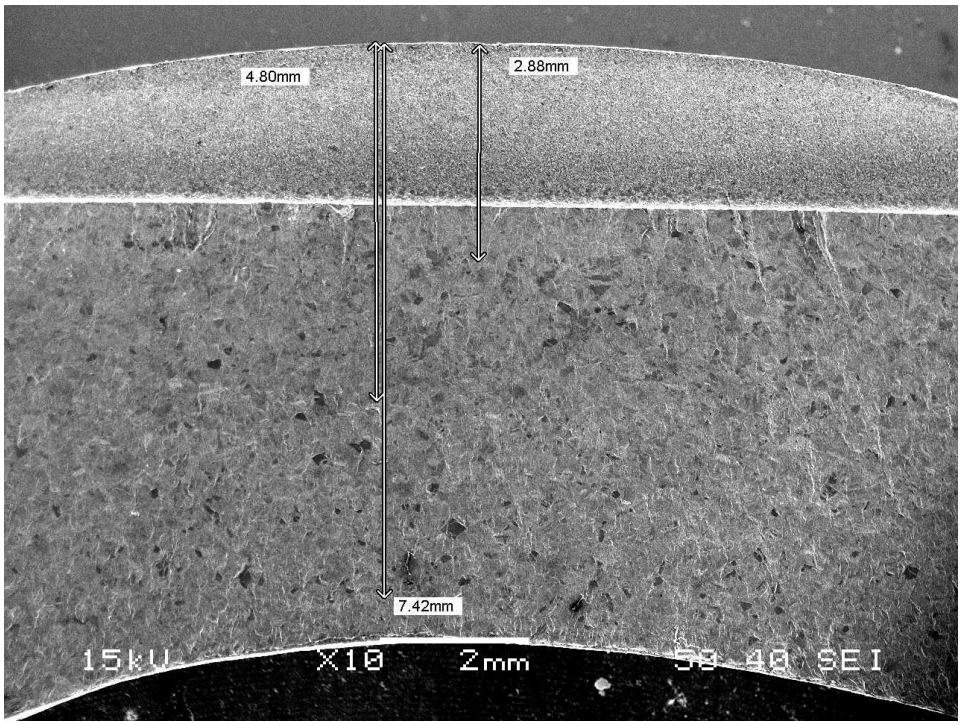

Fig. 4.1.2 SEM, Depth of cracks at three points

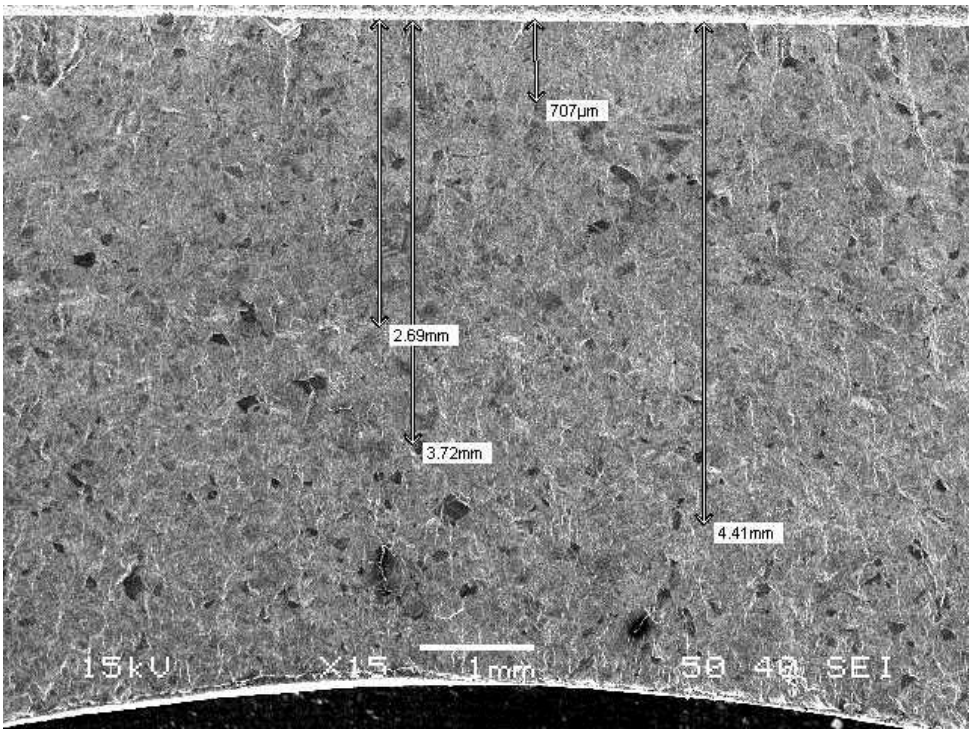

Fig. 4.1.3 SEM, Depth of cracks at different point to view Beach

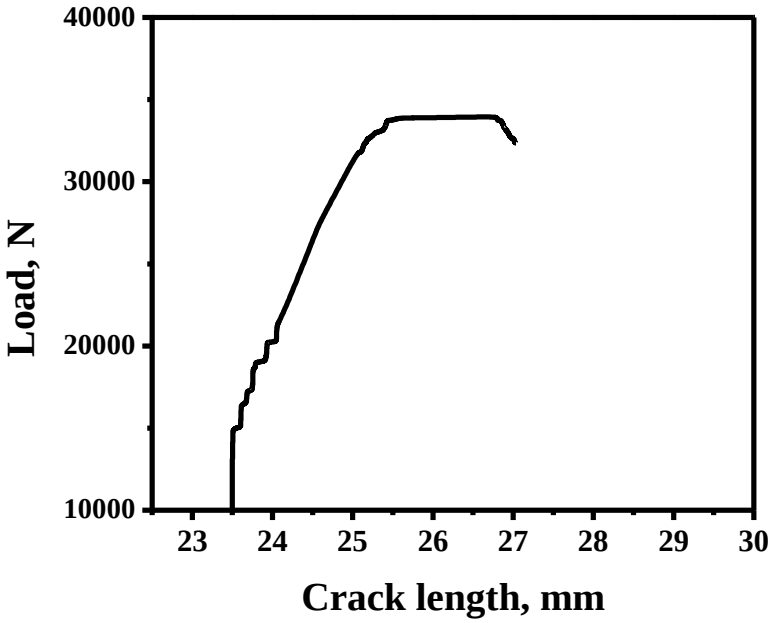

Fig. 4.1.4 (a) Load Vs. crack length for the pipe test

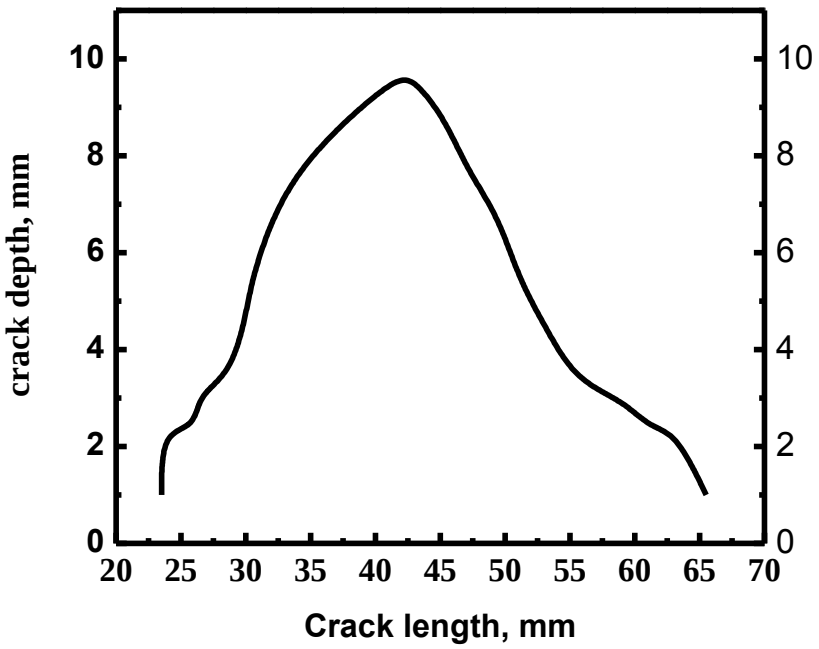

Fig. 4.1.4 (b) Crack shape at different interval of cyclic loading

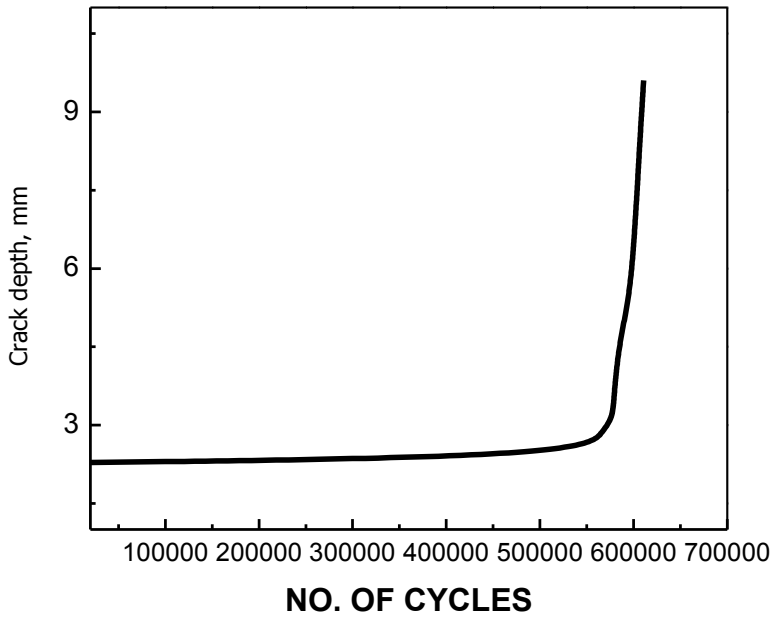

Fig. 4.1.4 (c) Max. Depth crack vs. number of cycles for different initial crack length

Chapter 5

FORMULATION AND VALIDATION OF MODEL

5. FORMULATION AND VALIDATION OF MODEL

5.1. Formulation of Model

Gamma function is a variant of factorial function with its arguments shifted by 1. That is if *n* is a positive integer then:

$$\Gamma (n) = (n-1)!$$

The Gamma function is defined for every complex number whose real part is positive and greater than zero. Generally it is given by an integral as mentioned below:

$$\Gamma(z) = \int_0^\infty t^{z-1} e^{-t} dt \ , \text{Re}\ (z) > 0.$$

Proposed model is a modification of the Gamma function. Here *t* is equal to number of cycles *N* and it is assumed to *w*. The parameter *z* was chosen in such a way that it becomes a non-dimensional parameter yet representing the properties that affect crack growth.

Since the integral is finite the value of integral is not *Γ (z)*. The integral was assumed to be equal to a non-dimensional parameter representing crack growth at the end of fixed cycles of loading. Generally fatigue crack growth depends on the initial crack length material properties and loading conditions etc. The non-dimensional parameter was chosen to include all those properties. So the formula for predicting the final crack length at the end of cycle is given as

$$\frac{ma_1}{w} = \int_0^N N^{\left(\frac{ma_0}{w}-1\right)} e^{-N} dN$$

Here *m* is a non-dimensional parameter whose value is approximately constant for a small interval of time. At first the value of *m* on RHS and LHS were considered different say m_1 on LHS and m_2 on RHS. The values of a_0, *w*, a_1, *N* were given as input is made fixed for a particular interval of cycles. The value of m_1 is input every time and value of m_2 was computed every time. The value of m_1 at which m_1 nearly becomes equal to m_2 was considered as the value of *m* for the interval.

$$\frac{m_2 a_1}{w} = \int_0^N N^{(\frac{m_1 a_0}{w}-1)} e^{-N} dN.$$

Here *m* stands, is a non-dimensional parameter expressed as

$$m = \left(\frac{E}{\sigma_{ys}} \times \frac{K_c}{\Delta K} \times \frac{K_{min}}{K_{max}}\right)^e$$

The value of *m* reduces with increase in the value of Δ*K*. The value of *m* changes with change in loading condition as well as crack length. Hence it was needed to correlate parameter *m* with parameters like two crack driving forces Δ*K* and K_{max} and with the material parameters such as plane stress fracture toughness (K_C), modulus of elasticity (*E*) and yield stress (σ_{ys}).

Fatigue crack growth depends on both Δ*K* and K_{max} in order to consider effects of mean stress. Since the modeling covers region III the value of fracture toughness (K_C) has to be considered. Crack growth also depends upon the material parameters like yield stress (σ_{ys}), Young's Modulus (*E*) and Ultimate strength (σ_{ut}). The parameter *m* is dimensionless and has a decreasing trend. So the value of *m* is correlated with dimensionless quantities like (*E*/ σ_{ys}), (K_C / Δ*K*), ($\frac{K_{min}}{K_{max}}$).

Here *e* for each cases has different so after some permutations it was found that the value of *e* critically depends ΔK_i and K_c so *e* is expressed by following polynomial in terms of ΔK_i and K_c.

$$e_i = C_0 + C_1 u_i + C_2 {u_i}^2 + C_3 {u_i}^3 + C_4 {u_i}^4 + \ldots \quad (6)$$

Where $u_i = (\frac{K_c}{\Delta K_i})$ .... (7)

Here *e* is varying with increasing **ΔK**

The value of *e* for each case has been shown in Table 5.1 as *e* different hence it must depend on certain properties which vary from one specimen to other. After some permutations it was found that the value of *e* depends upon the material parameters like ultimate strength (σ_{ut}) and the Young's (*E*) of the material. It was found that the ratio of the values of *e* depends upon the ratio $(\frac{K_c}{\Delta K_i})$. The values of *e* were compared and calculated. It was found that the value of *e* satisfies following formula for starting set of values is:

$$e = C\sqrt{\frac{\sigma_{ut}}{E_1}}$$

Where C= Constant

The logic behind this thing is as the specimen gets harder and harder the value of exponent is decreasing.

5.2. Validation of Model

We have data till four sets and we are validating for crack depth for fifth set. The validated graph are shown in Figure 5.2.1and Figure 5.2.2 It seems to γ-model has closer value with experimental result compare to Simpson 1/3rd rule.

Sol: Step1> $\boldsymbol{u_i = \left(\frac{360}{53.44}\right) = 6.736}$ from equation (2) then respective u_i values putting in eqn (1) and taking four sets of starting values of e_i and by the Mat LAB programme to finding coefficients, since we have

Step 2>

u1=[6.736 45.373696 305.6372163 2058.772289];
e=[.44 .404 .387 .359];
c=polyfit(u1,e,4)
f=polyval(c,u1)

C =

-2.32579401153935e-09 (C_4)5.61892525179909e-06(C_3)

-0.0017473457269968 1(C_2) 0.0768365453441470(C_1)

0(C_0)

f=0.4400 0.4040 0.3870 0.3590

Step3>

After putting all values of four coefficients you can get the value of *e*

Step>4

Here after getting coefficients you can pick value from *f* of polyval. Say *e* **(0.3590)**

Step 5>

Find the value of non-dimension no *m* by keeping exponent from *f.*

Step 6>

Find [(m*a/w)-1], here m_4**= 8.608** and use gamma function programme :

>> sysm x;

*>>int((x.^2.70).*exp(-x),0,10000)*

*ans = (3213*gamma(7/10))/1000 - (10002700459*10000^(7/10))/(100*exp(10000)) - (3213*igamma(7/10, 10000))/1000*

Here copy the real part and again enter in MatLAB it will give you $(m_4 * a_5/w)$ = **4.1707 s**o to get next depth of crack by formula

$(m_4 * a_5/w)$ = 4.1707 so a_5**= 4.3606**

For getting next step of exponent value, above formula are satisfactory with to finding incremented depth of crack.

5.3. **C++ where Simpson's 1/3 Rule was applied whose code is given in the table below.**

```
//Program to calculate value of 'm'
#include<iostream>
#include<conio.h>
#include<math.h>
using namespace std;
int main()
{
      long double a1,w,m1,m2,a2,a,b,h,f,s0,s1,s2,a11;
      long double i,m;
      a1=2.2396;        //initial crack length
      a2=2.844;         //next crack length
      a=0.0;
      b=5000;           //number of cycles
      w=52.00;          //value of width
      cout<<"\nEnter the value of m1 :";
      cin>>m1;          //Value of m1
      m=10000000;
      h=(b-a)/m;
      s1=0;
      s2=0;
      //Simpson's 1/3 rule computation
      s0=powl(a,((m1*a1/w)-1))*expl(-a)+powl(b,((m1*a1/w)-1))*expl(-
b);
      for (i=1.0;i<m;i+=2.0)
      {
            a11=a+i*h;
            s1=s1+powl(a11,((m1*a1/w)-1))*expl(-a11);
      }
      a11=0;
      for(i=2.0;i<m;i+=2.0)
      {
            a11=a+i*h;
            s2=s2+powl(a11,((m1*a1/w)-1))*expl(-a11);
      }
      f=(h/3)*(s0+4*s1+2*s2);
      m2=f*w/a2;
      cout<<"\nThe value of m2 is :"<<m2;
      return(0);
}
```

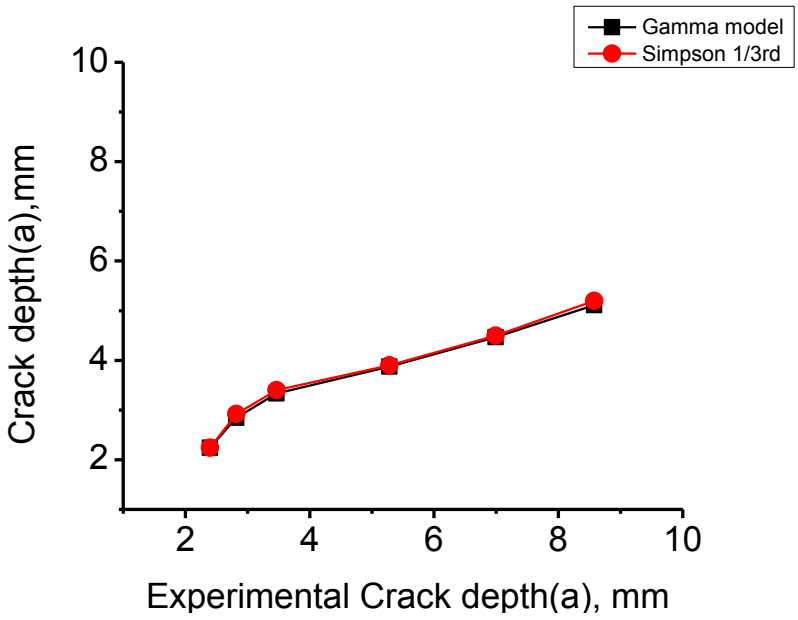

Fig. 5.2.1 Comparison of Gamma, Simpson 1/3rd and experimental crack depth

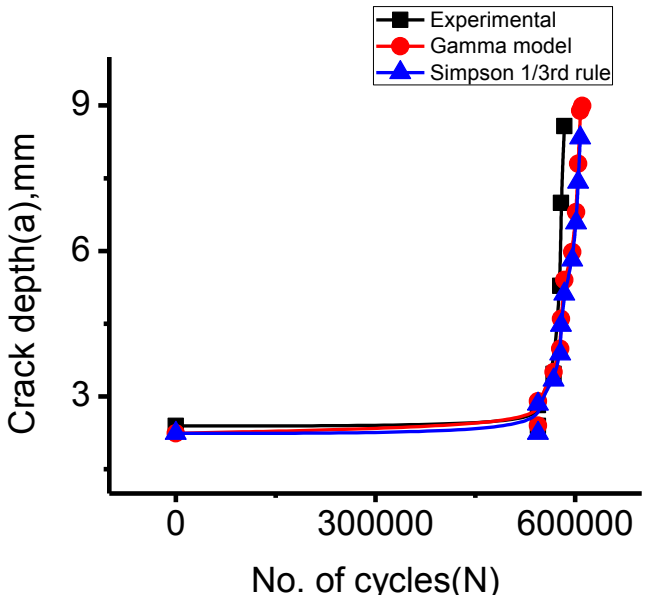

Fig. 5.2.2 Comparison of Gamma, Simpson 1/3rd and experimental number of cycles

The crack length in a body can be measured with the help COD gauge, electrical potential tool or by any other technique. This can also possible to predict that with the help of certain models. The γ-model with certain modification is attempted in this investigation the stress intensity factor at the crack tip has been followed for evaluating fatigue crack initiation with an assumption m_0 =15.391. Experimental and analytical results given in Table 4.1.1 and Table 5.2.1 for the pipes have been found to be in agreement, approximately. Experimental and analytical results are different may be due to the various assumptions made in the evaluation of fatigue crack initiation. Initiation of the crack is strongly dependent on the material condition, state of stress ahead of the crack tip and ahead of notch tip. It has also been found that for a given stress range, the number of cycles required for crack initiation is dependent on the initial crack depth. The stress intensity factor is less for a shallow crack than a deep crack for a given applied stress range. Therefore, local stress range ahead of the crack tip will be greater for a deeper crack than for shallow crack. This explains why the number of cycles required for initiation of cracking in pipes having a deep notch would be less in comparison to the pipe having a shallow notch. Experimental and analytical results for crack growth in the thickness direction have been observed to be in good agreement for all the pipes till *a/t* =0.4400**.**

The crack opening area associated with through-wall cracked pipes of stainless steel material loaded under pure bending is fairly approximated by the ellipse-shaped crack model. Large size flaws develop subcritical crack growth before the maximum moment is reached. This stable growth may be completely absent in pipes with small cracks. Crack depth from γ-model and Simpson $\frac{1}{3}$ rule are similar in nature but depth of crack in γ-model, increasing in smoothing manner which has been given in thesis. The following trends were observed when the graph was plotted for *m* by Mat LAB and Simpson $\frac{1}{3}$ rule with $\Delta \boldsymbol{K}$ for SS316L Alloy. It

seems to be the next incremented depth of cracks from Table 5.2.1 and Table 5.3.1, are in good agreement with the experimental results for the Pipe.

Table 5.2.1 Crack depth by the help of Mat LAB results

Sl no	**a_a(Depth of Crack**	**m_0(1st assumption)**	**m_1 (from Gama model)**	**m_{01}(mean)**	**e(varying for diff ΔK)**
1	2.2396	15.391	15.401	15.396	0.44
2	2.844	11.866	11.835	11.86	0.404
3	3.336	10.06	10.03	10.045	0.387
4	3.876	8.637	8.603	8.62	0.359
5	4.466	7.53	7.518	7.524	0.34
6	5.111	6.532	6.532	6.532	0.319
7	5.814	5.743	5.77	5.756	0.3
8	6.581	5.073	5.114	5.096	0.282
9	7.418	4.489	4.506	4.497	0.263
10	8.333	3.997	4.023	4.01	0.245
11	9.33				

Table 5.3.1 Crack depth by the help of Simpson $\frac{1}{3}$ rule results

Sl no	**Crack depth a_a (mm)**	**m_0(1st assumption)**	**m_1 (from Simsons 1/3rd rule model)**
1	2.2396	15.391	15.399
2	2.854	11.866	11.927
3	3.536	10.06	10.017
4	3.886	8.637	8.6
5	4.481	7.53	7.665
6	5.132	6.532	6.527
7	5.911	5.743	5.77
8	6.13	5.073	5.116
9	7.458	4.489	4.504
10	8.533	3.997	4.026
11	9.42		

Chapter 6

CONCLUSIONS

6. CONCLUSIONS

- γ-model of the form $\frac{ma_1}{w} = \int_0^N N^{(\frac{ma_0}{w}-1)} e^{-N} dN,$ can be effectively used to determine the next crack depth without going through numerical integration for TWC seamless stainless Pipes .

- γ-model has also applied on single edge notch (tension) SENT specimen by a group of B.Tech students and the results are in good agreement with the experimental observation.

- The Simpson 1/3rd rule is also applied to predict crack length of the pipe however it is found inferior than previous one.

Chapter 7

FUTURE WORK

7. FUTURE WORK

- Experimentation may be done using large number of sample for better accuracy and refinement of the proposed models.
- Elbows are important components in any piping system. The model may be developed for piping too.
- The experimentation may be conducted using notches of different shapes.

Chapter 8

LIST OF CONFERENCES

[1] International Conference: Shashi Kumar, P. K Ray, B.B Verma, *"Development of Compliance correlation for through wall cracked pipes"*, Advances in analytical Technique And Characterization of materials at RDCIS Ranchi (ATCOM), July 5-7-2011.

[2] National conference: Shashi kumar, J.R Mohanty, P.K Ray, *"Evaluation of fatigue crack growth and residual life using an exponential model",* 22nd Annual General meeting Materials research society of India held at Bhopal, Feb 14-16-2011.

[3] Student's Seminar on Metallurgical Engineering: Shashi kumar*, "Fatigue life Estimation using an Exponential model",* held at CSIR-National Metallurgical Laboratory, Jamshedpur, 25-26 March 2011.

Chapter 9

REFERENCES

9. REFERENCES

[1] MSE 2090: *"Introduction to Materials Science*", Chapter 8, Faliure.

[2] Denton, N.L., Magill, M.A., Hillsman, V.S., Roach, H.R., Thelen, R.K. (2000). *"Strength of Materials Laboratory Manual"*. West Lafayette, IN: Learning Systems Incorporated.

[3] Shigley, J.E, Mischke, C.R., (1989), *"Mechanical Engineering Design (6th ed.)",* N.Y., New York: McGraw-Hill.

[4] Mott, R.L. (2001). *"Applied Strength of Materials (4th ed.)".* Englewood Cliffs, NJ: Prentice Hall.

[5] A16. *"Guide for defect assessment and leak before break analysis"* (Third draft-December 31, 1995).

[6] Kunert, H. G. and Otegui, J. L., *"Factors Influencing Transit Fatigue of Seamless Pipes,"* Fatigue Fract. Eng. Mater. Struct., Vol. 28, 2005, pp. 455–466.

[7] Bruno, T. V., *"How to Prevent Fatigue to Tubular Goods,"* Standardiztion Confernce fo the Production Department, American Petroleum Institute, New Orleans, LA, 1987, http:// www.metallurigical.com/Publications/ Publication%2022.pdf.

[8] Jaske, C. E., *"The Effect of Cathodic Polarization on Fatigue Behavior,"* Proceedings of the Annual Conference and Exhibition on Corrosion, Paper No. 03243, San Diego, CA, 2003, NACE, Houston, TX.

[9] Ellyin F, Li HP. *"Fatigue crack growth in large specimens with various stress ratios".* J Pressure Vessel Technol 1984;106:255–60.

[10] Shibata K, Isozaki T, Ueda S, Kurihara R, Onizawa K, Kohsaka A. *"Results of reliability test program on light water reactor piping"*. Nucle Engg Des 1994;153:71–86.

[11] Yeon-Sik Y, Ando K. *"Circumferential fatigue crack growth and crack opening behavior in pipe subjected to bending moment"*. SMIRT-15, Seoul, Korea 1999;.

[12] Vosikovsky, O., *"Fatigue Crack Growth in X65 Line-Pipe Steel at Low Cycles Frequencies in Aqueous Environments,"J. Eng. Mater. Technol.*, Vol. 97, 1975, pp. 298–304.

[13] Vosikovsky, O. and Rivard, A., *"Growth of Surface Fatigue Cracks in Steel Plate," Int. J. Fatigue*, Vol. 3, 1981, pp. 111–115.

[14] Vosikovsky, O., *"Effect of Stress Ratio on Fatigue Crack Growth Rates in X70 Pipeline Steel in Air and Saltwater," J. Test. Eval.*, Vol. 8, No. 2, 1980, pp. 68–73.

[15] Vosikovsky, O., *"Fatigue Crack Growth in X70 Line-Pipe Steel in Sour Crude Oil," Corrosion (Houston)*, Vol. 32, No. 12, 1976, pp. 472–475.

[16] Shi, Y. W., Chen, B. Y., and Zhang, J. X., *"Effects of Welding Residual Stresses on Fatigue Crack Growth Behavior in Butt Welds of a Pipeline Steel," Eng. Fract. Mech.*, Vol. 36, 1990, pp. 893–902

[17] Xiong, Q. R., Zhuang, C. J., Feng, Y. R., Li, L. K., and Huo, C. Y., *"Experimental Studies on Fatigue Crack Growth Characteristics of X65 SSAW Pipe,"* Proceedings of the Seventh International Fatigue Congress, Beijing, China, June 8–12, 1999, EMAS,Wartley, UK.

[18] Hagiwara, N., Masuda, T., and Oguchi, N., *"Effects of Prestrain on Fracture Toughness on Fatigue-Crack Growth of Line Pipe Steels," J. Pressure Vessel Technol.*,Vol. 123, 2001, pp. 355–361.

[19] Tada, H., Paris, P. C., and Irwin, G. R., The Stress Analysis of Cracks Handbook, 3rd ed., American Society of Mechanical Engineers, NewYork, NY, 2000.

[20] ASTM Standard E647-05, 1998, *"Standard Test Method for Measurement of Fatigue Crack Growth Rates,"* Annual Book of ASTM Standards, Vol. 03.01, ASTM International, West Conshohocken, PA.

[21] Carter DK, Canda WR, Blind JA. *"Experimental evaluation of stress intensity factor for surface flaw growth in plates".* Surface crack growth models, experiments and structures. ASTM/STP 1060, Philadelphia: American Society for testing and Materials; 1990. p. 215–36.

[22] Nam WK, Fujibayashi S, Kotoji A, Nobukazu O. *"The fatigue life and fatigue crack through-thickness behaviour of a surface cracked plate"*. JSME Int J, Ser I 1988;31(2):272–9.

[23] Yeon-Sik Y, Ando K. *"Circumferential fatigue crack growth and crack opening behavior in pipe subjected to bending moment".* SMIRT-15, Seoul, Korea 1999.

[24] Chattopadhyay, J., Dutta, B.K., Kushwaha, H.S., 2004c. New 'η_{pl}' and 'γ' functions to evaluate J–R curves from cracked pipes andnelbows: part I—theoretical derivation. Eng. Fract. Mech. 71, 2635–2660.

[25] Zahoor, A., Kanninen, M.F., 1981. *"A plastic fracture mechanics prediction of fracture instability in a circumferentially cracked pipe in bending—part I:"* J-integral analysis. J. Press. Vess. Technol., Trans. ASME 103, 352–358.

[26] Bergman, M. (1995). *"Stress intensity factors for circumferential surface cracks in pipes".* Fatigue and Fracture of Engineering Materials and Structures 18, 1155–1172.

[27] Carpinteri, A. and Brighenti, R. (1998). *"Circumferential surface flaws in pipes under cyclic axial loading".* Engineering Fracture Mechanics 60, 383–396.

[28] Jones, R., Peng, D., Pitt, S. and Wallbrink, C. (2004). Weight functions, CTOD, and related solutions for cracks at notches. Engineering Failure Analysis 11, 79–114.

[29] Peng, D. (2002). *"Methods for failure assessment of structures and applications to shape optimization".* In: Mechanical Engineering, Monash University, Melbourne.

Chapter 10

APPENDIX A

10.APPENDIX

a. Calculation for Straight Pipe

The loads applied to the specimens were defined by either a constant stress range (σ_r) or constant stressamplitude (σ_a).

$$\sigma_r = \sigma_{max} - \sigma_{min} = 241\ Mpa$$

$$\sigma_a = \frac{\sigma_r}{2} = 120\ Mpa$$

$$\sigma_m = \frac{\sigma_{max} + \sigma_{min}}{2} = 132.5\ Mpa$$

$$R = \sigma_{min/\sigma_{max}} = .1$$

Where σ_{max} and σ_{min} are maximum and minimum cyclic stress respectively.

$\frac{\sigma}{Y} = \frac{M}{I} = \frac{E}{R}$ From here we find $M = P*a$

Also we have

$K = \sigma\sqrt{\pi * R * (\theta)} * F(\theta)$

Where

$\theta = 0.392\ rad$ when Θ = 22.5

$F(\theta) = 1 + 6.8(\theta/\pi)^{1.5} - 13.6(\theta/\pi)^{2.5} + 20.0(\theta/\pi)^{3.5} = 1.239$

Also $2\theta = 45^{\circ}, 60^{\circ}, 90^{\circ}, 100^{\circ}$ *here* $2\theta < 110^{\circ}$

So $K_{max} =$ 48.06231393 Mpa

R = 21 mm

Δk = 43.25608254 Mpa

b. C++ where Simpson's 1/3 Rule was applied whose code is given in the table below.

```
//Program to calculate value of 'm'
#include<iostream>
#include<conio.h>
#include<math.h>
using namespace std;
int main()
{
      long double a1,w,m1,m2,a2,a,b,h,f,s0,s1,s2,a11;
      long double i,m;
      a1=2.2396;        //initial crack length
      a2=2.844;         //next crack length
      a=0.0;
      b=5000;           //number of cycles
      w=52.00;          //value of width
      cout<<"\nEnter the value of m1 :";
      cin>>m1;          //Value of m1
      m=10000000;
      h=(b-a)/m;
      s1=0;
      s2=0;
      //Simpson's 1/3 rule computation
      s0=powl(a,((m1*a1/w)-1))*expl(-a)+powl(b,((m1*a1/w)-1))*expl(-
b);
      for (i=1.0;i<m;i+=2.0)
      {
            a11=a+i*h;
            s1=s1+powl(a11,((m1*a1/w)-1))*expl(-a11);
      }
      a11=0;
      for(i=2.0;i<m;i+=2.0)
      {
            a11=a+i*h;
            s2=s2+powl(a11,((m1*a1/w)-1))*expl(-a11);
      }
      f=(h/3)*(s0+4*s1+2*s2);
      m2=f*w/a2;
      cout<<"\nThe value of m2 is :"<<m2;
      return(0);
}
```

MATLAB sample program

>> sysm x;

*>>int((x.^2.70).*exp(-x),0,10000)*

*ans = (3213*gamma(7/10))/1000 - (10002700459*10000^(7/10))/(100*exp(10000)) - (3213*igamma(7/10, 10000))/1000*

Here copy the real part and again enter in MatLAB it will give you $(m_4 * a_5/w)$ **= 4.1707**

to get next depth of crack by formula

$(m_4 * a_5/w)$ = 4.1707 so a_5**= 4.3606(Ans)**